JOURNAL OF CATALYSIS 145, 251–255 (1994)

A Study by ^{31}P NMR Spin Echo Mapping of VPO Catalysts

I. Characterization of the Reference Phases

M. T. Sananes,[1] A. Tuel, and J. C. Volta

Institut de Recherches sur la Catalyse, CNRS, 2 Avenue A. Einstein, 69626, Villeurbanne, Cédex, France

Received June 17, 1993; revised August 26, 1993

Spectra of ^{31}P NMR by spin echo mapping of the pure VPO phases and the corresponding precursors are presented. They show that it is possible to distinguish phases in the V^{4+} and V^{5+} oxidation states, as has been previously published. In addition, the technique can characterize a V^{3+} phase. Evidence of dispersed V^{5+} on the VPO matrix is presented. © 1994 Academic Press, Inc.

INTRODUCTION

Vanadium–phosphorus oxides (VPO) are well known catalysts for the oxidation of *n*-butane to maleic anhydride (MA). An entire issue of *Catalysis Today* was recently devoted to this topic (1). The investigation of the mechanism of reaction and nature of the active sites is a work in progress, and knowledge of the VPO system is rapidly evolving. The fact that the vanadyl pyrophosphate $(VO)_2P_2O_7$ is the active phase is well known, but most published data refer to a mean bulk composition that does not exclude the formation of an equilibrium V^{4+}/V^{5+} on the surface of vanadyl pyrophosphate during butane oxidation. From comparison of the evolution of catalytic performance with classical ^{31}P MAS–NMR data, we emphasized the importance of a specific V^{4+}/V^{5+} ratio located in the basal (100) $(VO)_2P_2O_7$ face for the best results (2). The valence state of vanadium in the active surface is thus highly important, and it appears that the addition of phosphorus is able to control this parameter by preventing the oxidation of vanadyl pyrophosphate to $VOPO_4$ (3). From an industrial point of view, a distinction is made between a nonequilibrated (short-term catalytic test) and equilibrated (long-term catalytic test) catalyst, and it is shown that the C_4/air mixture tends to result in a changing of the V^{4+}/V^{5+} ratio from one to the other in such a way that the rate of V^{4+} oxidation to V^{5+} tends to decrease for the equilibrated catalyst. It was pointed out that this specific topic requires further investigation since the changes occurring in the VPO catalyst during reaction are directly connected to the catalytic performance (1). When increased C_4/air ratios are used, it is possible to detect the formation of an intermediate olefin from *n*-butane. In this case, some V^{3+} is detected in the VPO catalyst (4).

As a matter of fact, it appears that direct knowledge of the oxidation state of vanadium, using a physicochemical technique, is highly important to control the selectivity of the reaction. Indeed, the results of the titration of the valence state of vanadium which implies a chemical dissolution by sulfuric acid should be considered with caution.

The idea that typical industrial catalysts contain V^{4+} and V^{5+} has been supported by ^{31}P NMR spin echo mapping (6). Indeed, because of the presence of paramagnetic centers in these materials, conventional NMR studies of VPO catalysts have been limited. These centers not only affect the ability to obtain ^{51}V NMR spectra, but also the spectra of the neighbouring ^{31}P nuclei. However, the shift and linewidth modification of ^{31}P NMR signals due to the presence of paramagnetic ions have been used to examine the oxidation state of the vanadium centers by using the spin echo mapping technique (6).

Typically, two major peaks were observed in the spectra of industrial catalysts as previously published (6): one around 0 ppm, corresponding to phosphorus atoms in the vicinity of V^{5+} ions, and one at about 2500 ppm, due to the proximity of V^{4+} centers. These peaks could be very broad and overlap so that NMR lines extending from 0 to 4000 ppm were sometimes observed. However, no interpretation of intermediate lines (around 1000 ppm) was reported.

Moreover, the use of the spin echo mapping technique for the possible observation of V^{3+} ions was not mentioned. In the present publication, we report the characterization of pure reference phases with the V^{3+}, V^{4+}, and V^{5+} oxidation states by ^{31}P NMR using the spin echo mapping technique.

[1] On leave from INCAPE-Santa Fe/Argentina.

0021-9517/94 $5.00

EXPERIMENTAL

The preparation of the three precursors of the VPO phases, namely, $NH_4(VO_2)_2PO_4$, $VOPO_4 \cdot 2H_2O$, and $VOHPO_4 \cdot 0.5H_2O$, has been published elsewhere as for the pure α_I, β, γ, and δ $VOPO_4$ phases (V^{5+} phases) (7–11). $(VO)_2P_2O_7$ (V^{4+} phase) was prepared by calcination at 750°C of $VOHPO_4 \cdot 0.5H_2O$ under nitrogen for 100 h. Three sets of experiments were conducted in the same furnace with different masses of solids.

The conditions of preparation of $VO(H_2PO_4)_2$, usually called phase E (12) and used as the precursor for the $VO(PO_3)_2$ phase (V^{4+} phase), have been reported (8). $VO(PO_3)_2$ was obtained by calcination of phase E at 500°C under different conditions which are later discussed.

VPO_4 (V^{3+} phase) (14) was obtained by reduction of $(VO)_2P_2O_7$ under 5% hydrogen/argon using a linear increase of temperature from 25°C up to 900°C.

The purity of all the VPO phases was monitored by X-ray diffraction, ^{31}P MAS–NMR, and Raman spectroscopy. Their characteristics were in agreement with previously published results (10–14).

All ^{31}P NMR experiments were performed on a Bruker MSL 300 NMR spectrometer. Conventional spectra were obtained at 121.5 MHz using a 90°x-(acquire) sequence. The 90° pulse was 4.2 μs and the delay time between two consecutive scans was 10 s. Samples were typically spun at 4 kHz in zirconia rotors using a double bearing probehead.

The ^{31}P spin echo spectra were recorded under static conditions, using a 90° x-τ-180°y-τ-(acquire sequence). The 90° pulse was 4.2 μs and τ was 20 μs. For each sample, the irradiation frequency was varied in increments of 100 kHz above and below the ^{31}P resonance of H_3PO_4. The number of spectra thus recorded was dictated by the frequency limits, beyond which no spectral intensity was visible. The ^{31}P NMR spin echo mapping information was then obtained by superposition of all spectra. Some additional UV–visible and ESR experiments were conducted in order to control the presence of vanadium with different oxidation states. UV–visible spectra were recorded on a Perkin–Elmer Lambda 9 spectrometer equipped with an integration sphere. ESR spectra were recorded at room temperature with a Varian E9 spectrometer using 9.3-GHz (X band) microwave frequencies.

RESULTS AND DISCUSSION

Figure 1 gives the ^{31}P NMR spin echo mapping spectrum of two preparations of the $VOHPO_4 \cdot 0.5H_2O$ phase obtained by refluxing a suspension of V_2O_5 in isobutanol in the presence of 85% H_3PO_4 ($P/V = 1.1$) (10) which differed only by different times used to crystallize the phases. An intense peak is observed in both preparations at δ = 1625 ppm (Figs. 1a and 1b). The small peak at 0 ppm is characteristic of phosphorus atoms bonded to V^{5+} sites, as observed by ^{31}P MAS–NMR (10). The intense peak at 1625 ppm is characteristic of the PO_4 groups bonded to the V^{4+} cations of the hemihydrate structure (10). The shoulder observed in the 250–1000 ppm region for spectrum 1b appears to be connected to the crystallinity of the material, since the XRD pattern of the corresponding samples showed distinct relative intensities for the (001) and (220) reflections.

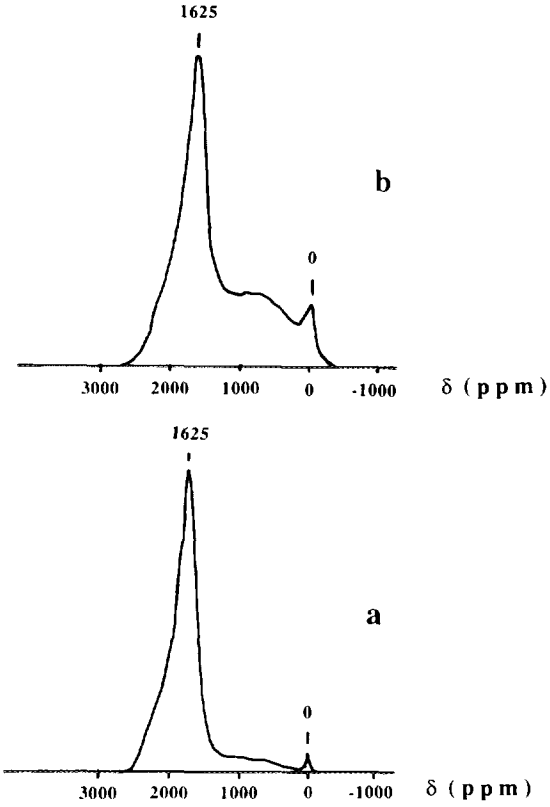

FIG. 1. ^{31}P NMR spin echo mapping of two preparations of the $VOHPO_4 \cdot 0.5H_2O$ hemihydrate.

The ^{31}P NMR spectrum by spin echo mapping of $VO(H_2PO_4)_2$, called phase E (15) (Fig. 2), exhibits an intense peak at 2300 ppm which is characteristic of phosphorus atoms bonded to the V^{4+} cations in a quite different environment as compared to the hemihydrate structure, since both structures are supposed to be very different (15).

Figure 3 presents the ^{31}P spin echo mapping spectra of the four α_I, β, γ, and δ $VOPO_4$ phases (V^{5+} phases). No differences were observed in the position of the single peak at 0 ppm as for the H_3PO_4 reference (11). However, the linewidths of γ and δ $VOPO_4$ were broader than those of α_I and β $VOPO_4$, in agreement with previous observations by classical ^{31}P MAS–NMR (10). No signals charac-

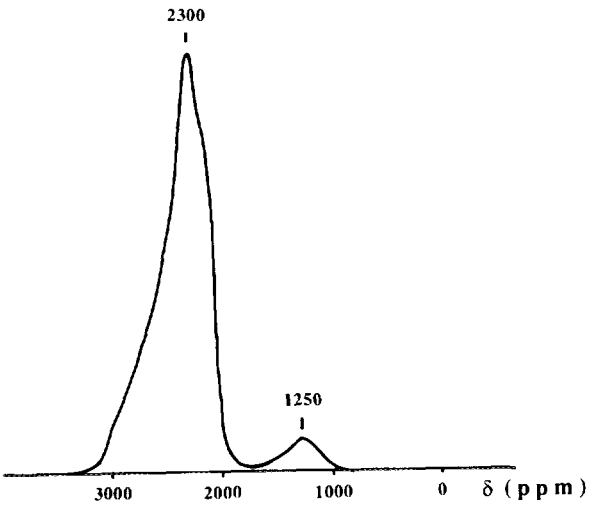

FIG. 2. ^{31}P NMR spin echo mapping of $VO(H_2PO_4)_2$ (phase E).

teristic of P bonded to V^{4+} cations could be detected in the 1500–2500 ppm range despite the observation of an ESR signal. This is probably due to the higher sensitivity of the V^{4+} detection by ESR as compared to the ^{31}P NMR by spin echo mapping technique. The detection of any signal around 0 ppm using the ^{31}P NMR by spin echo mapping does not allow the identification of the $VOPO_4$ phases. Additional experiments using X-ray diffraction, laser Raman spectroscopy, or classical ^{31}P MAS–NMR are thus necessary (11).

Figure 4 shows the spectra of solids obtained from calcination of phase E under different conditions. Figure 4a corresponds to a treatment under nitrogen at 500°C for 4 h. Poorly crystallized $VO(PO_3)_2$ was detected by XRD, in agreement with the broad signal observed on Fig. 4a. Figures 4b and 4c correspond to calcinations under air at 500°C for 4 and 20 h, respectively. $VO(PO_3)_2$ is still observed by XRD on both samples, with a better crystallinity as compared with the material obtained under nitrogen (Fig. 4a). Basically, the three spectra present the same

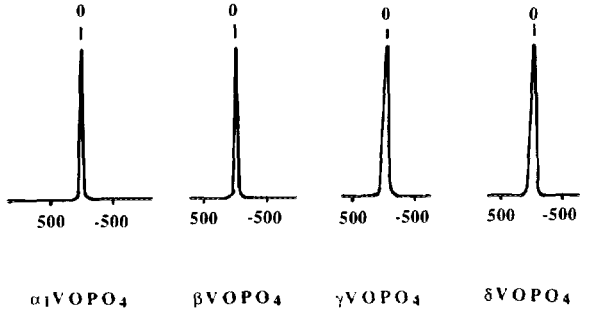

FIG. 3. ^{31}P NMR spin echo mapping of the α_I, β, γ, and δ $VOPO_4$ phases.

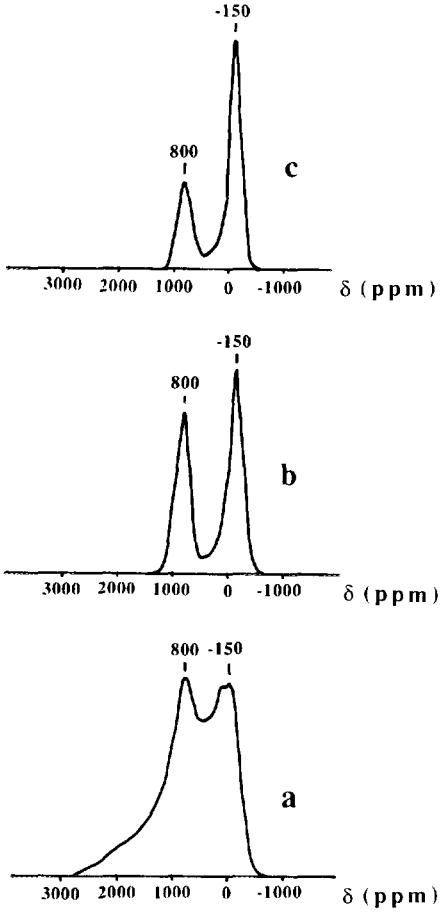

FIG. 4. ^{31}P NMR spin echo mapping of samples obtained by calcination of $VO(H_2PO_4)_2$ (phase E) at 500°C: (a) under nitrogen for 4 h, (b) under air for 4 h, and (c) under air for 20 h.

features with characteristic peaks at 800 and −150 ppm. The peak at −150 ppm which appears 150 ppm lower than the position normally observed for the $VOPO_4$ structures (0 ppm) has been attributed to P atoms bonded to V^{5+} species in a strong interaction with the $VO(PO_3)_2$ structure, while the peak at 800 ppm was considered as characteristic of P atoms bonded to the V^{4+} atoms of the $VO(PO_3)_2$ structure. It thus appears that the conditions of treatment (N_2 or air) and the duration of calcination strongly influence the relative distribution of the 800 and −150 ppm peaks. This result emphasizes the interest of ^{31}P spin echo mapping to reveal an evolution of the V^{4+} distribution with the conditions of treatment. It appears normal to observe an increase of the V^{5+} contribution from the nitrogen treatment to the air treatment and with the duration. The classical ^{31}P MAS–NMR of the corresponding solids showed a characteristic spectrum with a very broad signal centered at −150 ppm (Fig. 5).

Figure 6 presents the spectrum of VPO_4 (V^{3+} phase). A single broad peak is observed at about 4650 ppm. No

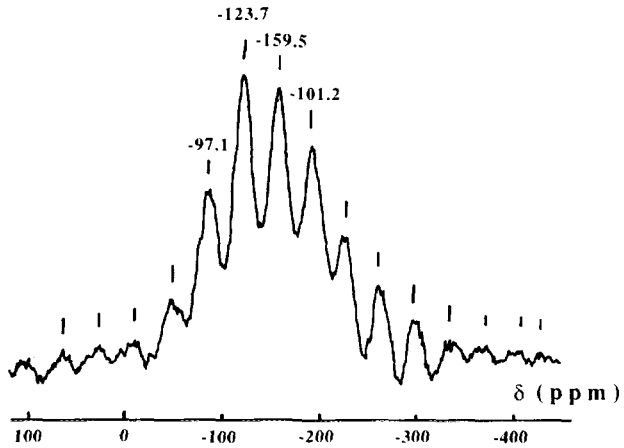

FIG. 5. ^{31}P MAS-NMR spectrum of the sample obtained after calcination of $VO(H_2PO_4)_2$ (phase E) at 500°C under nitrogen for 4 h (sample corresponding to Fig. 4a).

signals was observed around 2000 and 0 ppm, evidencing that the material did not contain any V^{4+} and V^{5+} phases. Therefore, such a chemical shift can be unambiguously attributed to V^{3+} cations in VPO_4. This result is very important, since it is the first evidence of V^{3+} ions in VPO systems using solid-state NMR. The high chemical shift for this phase as compared to the V^{4+} phases is not surprising. Indeed, addition of an electron to V^{5+} (which has a $3d^0$ configuration) shifts the ^{31}P NMR signal from about 0 ppm to the 1500–2500 ppm region, depending on the nature of the phase. When a second electron is present on the outer electronic layer of the V center (V^{3+} with a $3d^2$ configuration), electronic effects are more important and the ^{31}P NMR peaks are expected to be in the spectral region above 3000 ppm if V^{3+} cations are paramagnetic centers. Taking into account that VPO_4 is obtained after reduction of $(VO)_2P_2O_7$ and assuming that the chemical

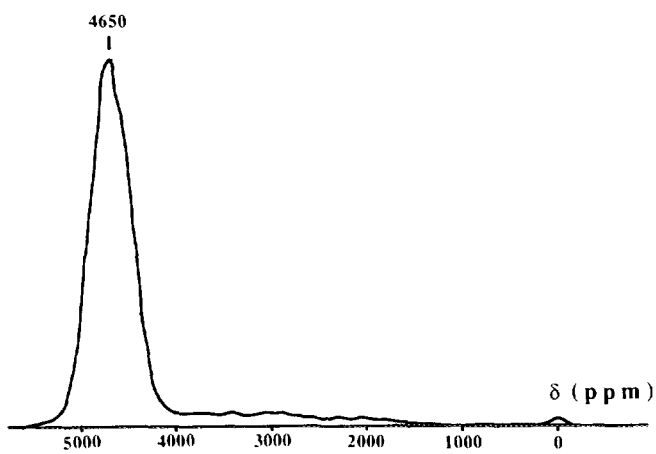

FIG. 6. ^{31}P NMR spin echo mapping of VPO_4.

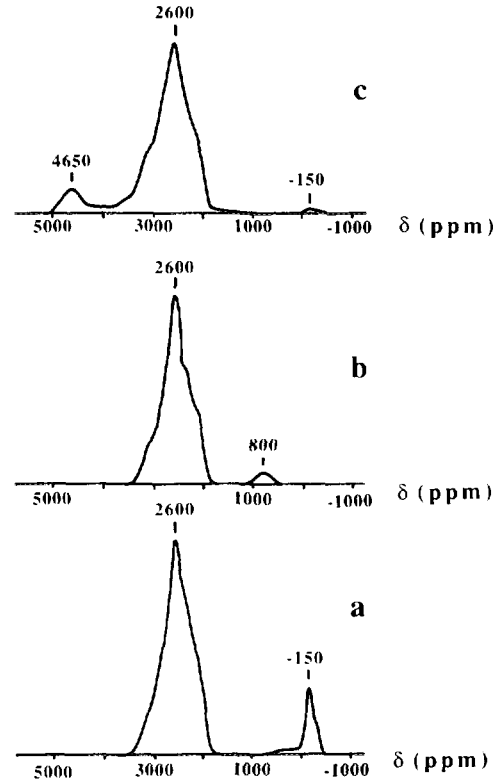

FIG. 7. ^{31}P NMR spin echo mapping of samples obtained by calcination at 750°C under nitrogen of $VOHPO_4 \cdot 0.5H_2O$ for 100 h.

shift is proportional to the electron nuclear interaction (6), one should expect a line between 4000 and 6000 ppm, which is observed experimentally.

Figure 7 presents the spectrum of $(VO)_2P_2O_7$ (V^{4+} phase) on three different preparations obtained by calcination at 750°C under nitrogen of the same $VOHPO_4 \cdot 0.5H_2O$ precursor for 100 h. The precursor was heated from 25 up to 400°C at a heating rate of 3°C/min, kept 1 h at 400°C, then heated from 400 up to 750°C at 5°C/min, and finally kept at 750°C for 100 h. The only difference between the three preparations was the mass of the treated precursor, i.e., 1.5 g for Fig. 7a, 2.0 g for Fig. 7b, and 3.0 g for Fig. 7c. It clearly appears that the three spectra are very different. They show a common feature with a characteristic peak at 2600 ppm which is assigned to P atoms bonded to V^{4+} cations in the $(VO)_2P_2O_7$ structure, as previously observed (6). The differences observed are associated with the side peaks at −150 ppm for Fig. 7a, 800 ppm for Fig. 7b, and 4650 ppm for Fig. 7c. From the previous examinations (see Fig. 4), it is obvious that the peak at −150 ppm can be attributed to P atoms bonded to V^{5+} species in strong interaction with the $VO(PO_3)_2$ structure, while the peak at 800 ppm corresponds to P atoms bonded to the V^{4+} atoms of the $VO(PO_3)_2$ structure (Fig. 4). Finally, the peak at 4650 ppm is due to P atoms

bonded to some V^{3+} cations (Fig. 6), which evidences a slight reduction in this last case. Therefore, it can be seen that an increase in the mass of the precursor results in a reduction of the catalyst. Moreover, the increase of the linewidth in Figs. 7a and 7c as compared to Fig. 7b is in agreement with the loss of crystallinity as observed by XRD. This last study shows that the kinetics of water evolution, which is the only parameter which changes with the different masses of $VOHPO_4 \cdot 0.5H_2O$ used from one preparation to the other, strongly influences the distribution of V^{5+} and V^{3+} cations beside $(VO)_2P_2O_7$ (V^{4+}) which are not detected by XRD as characteristic V^{5+} and V^{3+} phases, respectively. This emphasizes the difficulty of reproducing the preparation of VPO reference phases with the same purity if all parameters are not strictly controlled.

CONCLUSIONS

Three different oxidation states of vanadium can be directly distinguished by ^{31}P NMR by spin echo mapping of vanadium phosphate catalysts. All the $VOPO_4$ structures (phases in the V^{5+} oxidation state) give a common feature with a signal at 0 ppm characteristic of the PO_4 tetrahedron in H_3PO_4. For phases containing V^{4+}, signals depend strongly on the environment of the P atoms with the V atoms, and are spread over a quite large range. It is observed at 800 ppm for $VO(PO_3)_2$, at 2600 ppm for $(VO)_2P_2O_7$, at 1625 ppm for $VOHPO_4 \cdot 0.5H_2O$, and at 2300 ppm for $VO(H_2PO_4)_2$. For VPO_4 (phase in the V^{3+} oxidation state), the ^{31}P NMR spin echo mapping signal is observed at 4600 ppm.

We attempted to correlate the position of the ^{31}P NMR by spin echo mapping peaks to the different local environment of P with V atoms, considering the structure of the different V^{4+} phases, as published before (15). This was possible in the case of $VOHPO_4 \cdot 0.5H_2O$ and $(VO)_2P_2O_7$ but not for $VO(H_2PO_4)_2$ and $VO(PO_3)_2$. This can be explained by the fact that a correlation with the structure is difficult. It implies a correlation with the local bonding situation and particularly (a) to the total moment of the unpaired electron(s) and (b) to the fraction of unpaired electron spin density appearing at the nucleus of the ^{31}P.

Our ^{31}P NMR study by spin echo mapping showed also the possibility of detecting the presence of V^{5+} cations on the $VO(PO_3)_2$ matrix with a signal at -150 ppm. This information is highly important, since the dispersion of V^{5+} appears to be a controlling factor in the catalytic performance for butane oxidation to maleic anhydride (2).

From this study, it appears that the conditions of decomposition of the two precursors $VOHPO_4 \cdot 0.5H_2O$ and $VO(H_2PO_4)_2$ and thus the kinetics of H_2O evolution can control the oxidation state of vanadium which should have a strong influence on the catalytic activity. This point will be discussed in a forthcoming publication through the study of industrial VPO catalysts by ^{31}P NMR spin echo mapping with different durations of activation.

REFERENCES

1. Centi, G. (Ed.), "Vanadyl Pyrophosphate Catalysts," Catalysis Today, Vol. 16, No. 1. Elsevier, Amsterdam, 1993.
2. Zhang, Y., Sneeden, R. P. A., and Volta, J. C., *Catal. Today* **16,** 39 (1993).
3. Cornaglia, L. M., Caspani, C., and Lombardo, E. A., *Appl. Catal.* **74,** 15 (1991).
4. Centi, G., Fornasari, G., and Trifiro, F., *J. Catal.* **89,** 44 (1984).
5. Niwa, M., and Murakami, Y., *J. Catal.* **76,** 9 (1982).
6. Li, J., Lashier, M. E., Schrader, G. L., and Gerstein, B. C., *Appl. Catal.* **73,** 83 (1991).
7. Ladwig, G., *Z. Anorg. Allg. Chem.* **338,** 266 (1965).
8. Bordes, E., Courtine, P., and Pannetier, G., *Ann. Chim.* **8,** 105 (1973).
9. Souchay, P., and Dubois, S., *Ann. Chim.* **3,** 88 (1948).
10. Johnson, J. W., Johnston, D. C., Jacobson, A. J., and Brody, J. F., *J. Am. Chem. Soc.* **106,** 8123 (1984).
11. Ben Abdelouahab, F., Olier, R., Guilhaume, N., Lefebvre, F., and Volta, J. C., *J. Catal.* **134,** 151 (1992).
12. Hodnett, B. K., *Catal. Rev.-Sci. Eng.* **27**(3), 373 (1985).
13. Ladwig, G., *Z. Chem.* **8,** 307 (1968).
14. Tudo, J., and Carton, C., *C.R. Acad. Sci. Paris Ser C* **289,** 219 (1979).
15. Bordes, E., *Catal. Today* **1,** 499 (1987).